Numerical simulations of ultrasimple ultrashort-laser-pulse measurement

Xuan Liu and Rick Trebino

Georgia Institute of Technology, School of Physics, 837 State St, Atlanta, GA 30332 USA
xuan.liu@mail.gatech.edu

Arlee V. Smith

Sandia National Laboratories, Albuquerque, NM 87185, USA

Abstract: We numerically simulate the performance of the ultrasimple frequency-resolved-optical-gating (FROG) technique, GRENOUILLE, for measuring ultrashort laser pulses. While simple in practice, GRENOUILLE has many theoretical subtleties because it involves the second-harmonic generation of relatively tightly focused *and* broadband pulses. In addition, these processes occur in a *thick* crystal, in which the phase-matching bandwidth is deliberately made narrow compared to the pulse bandwidth. In these simulations, we include all sum-frequency-generation processes, both collinear and noncollinear. We also include dispersion using the Sellmeier equation for the crystal BBO. Working in the frequency domain, we compute the GRENOUILLE trace for practical—and impractical—examples and show that accurate measurements are easily obtained for properly designed devices.

OCIS codes: (320.7100) Ultrafast measurements; (190.7110) Ultrafast nonlinear optics.

References and links

1. R. Trebino, Frequency-Resolved Optical Gating: The Measurement of Ultrashort Laser Pulses (Kluwer Academic Publishers, Boston, 2002).
2. P. O'Shea, M. Kimmel, X. Gu, and R. Trebino, "Highly simplified device for ultrashort-pulse measurement," Opt. Lett. **26**, 932-934(2001).
3. C. Radzewicz , P. Wasylczyk and J. S. Krasinski, "A poor man's FROG," Opt. Comm. **186,** 329-333(2000)
4. S. Akturk, M. Kimmel, P. O'Shea, and R. Trebino, "Measuring pulse-front tilt in ultrashort pulses using GRENOUILLE," Opt. Express **11**, 491-501(2003).
5. S. Akturk, M. Kimmel, P. O'Shea, and R. Trebino, "Measuring spatial chirp in ultrashort pulses using single-shot Frequency-Resolved Optical Gating," Opt. Express **11**, 68-78(2003).
6. P. O'Shea, S. Akturk, M. Kimmel, and R. Trebino, "Practical issues in ultra-short-pulse measurements with 'GRENOUILLE'," Appl. Phys. B **79**, 683-691(2004).
7. S. Akturk, M. Kimmel, P. O'Shea, and R. Trebino, "Extremely simple device for measuring 20 fs pulses," Opt. Lett. **29**, 1025-1027(2004).

1. Ultrashort-laser-pulse device complexity and its reduction: GRENOUILLE

Measuring ultrashort laser pulses has traditionally been a difficult task. Virtually all available techniques are based on autocorrelation, which requires splitting the pulse into two replicas, recombining them in space and time in a nonlinear-optical medium, and measuring the nonlinear-optical signal pulse while varying the delay between the two replicas. Methods that yield more than the mere autocorrelation also require additional optics, such as a spectrometer, and some methods also involve devices as complex as interferometers and pulse shapers or stretchers, as well. Complex devices are inherently difficult to work with and are

#79262 - $15.00 USD Received 22 Jan 2007; revised 26 Mar 2007; accepted 27 Mar 2007; published 3 Apr 2007

usually easily misaligned. As a result, complex devices often introduce the very distortions they are designed to measure. While complex computer programs can also be required, this does not add complexity to the device operation, as, in the case of frequency-resolved-optical-gating (FROG), such programs are available commercially and are now also very reliable and fast. And computer programs do not misalign or change with time. Thus, *experimental* simplicity is the high priority of ultrashort-pulse measurement.

Recently, an extremely simple pulse-measurement device was introduced and is now in wide use. A highly simplified version of the FROG [1] family of devices, this method (called GRENOUILLE [2]; see Fig.1) operates by using a simple, large-apex-angle prism (a "Fresnel biprism") to split the beam into two replicas and to automatically cross and align them in space and time in the crystal. It uses a relatively large beam-crossing angle and a line focus, so the pulse replicas' relative delay is mapped onto the crystal transverse position (see Fig. 2(a)) yielding single-shot operation. GRENOUILLE's second innovation is the use of a thick second-harmonic-generation (SHG) crystal[2,3], which, due to its thickness, phase-matches only a small—and different—fraction of the pulse bandwidth for each output angle, allowing the crystal to operate, not only as an autocorrelating element, but also as the dispersive element of a spectrometer (see Fig. 2(b)). The phase-matching bandwidth of the thick crystal is then GRENOUILLE's spectral *resolution*—not its spectral *range*, as in other pulse-measurement devices. The spectral range is determined instead by the angular divergence of the beam.

These two innovations yield a very simple, compact FROG device composed of only four easily aligned, linearly arranged, optical elements and that requires almost no alignment and never misaligns. In addition, without modification, GRENOUILLE also measures the spatio-temporal distortions, spatial chirp and pulse-front tilt: the otherwise symmetrical trace develops shear in the presence of spatial chirp and displacement along the delay axis in the presence of pulse-front tilt[4, 5].

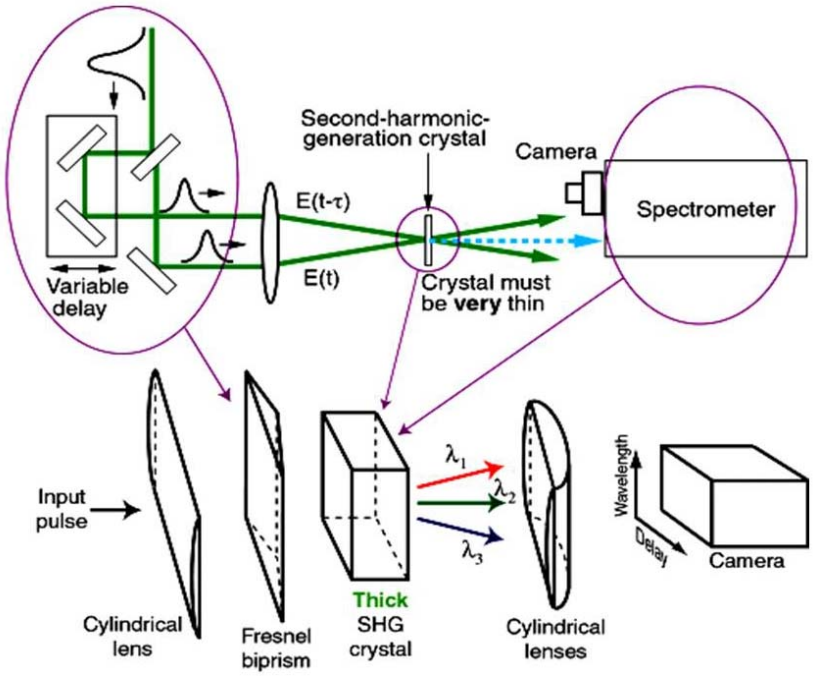

Fig. 1. (a). FROG (top) and its simpler cousin, GRENOUILLE (bottom). GRENOUILLE replaces the beam splitter and recombining apparatus with a Fresnel biprism. And it also replaces the thin crystal and spectrometer with a thick crystal.

#79262 - $15.00 USD Received 22 Jan 2007; revised 26 Mar 2007; accepted 27 Mar 2007; published 3 Apr 2007

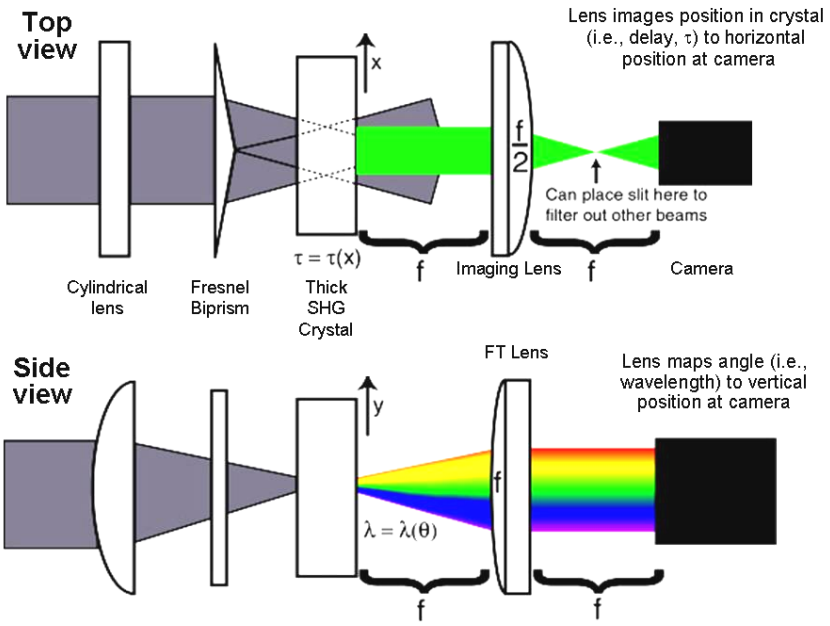

Fig. 1. (b). GRENOUILLE from above and the side.

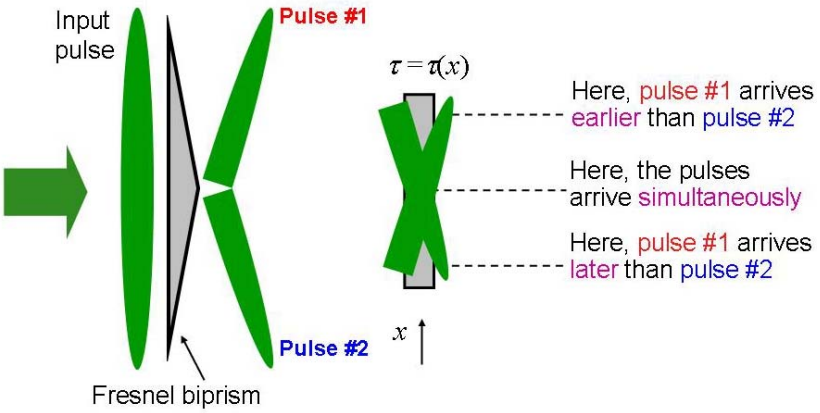

Fig. 2. (a). The Fresnel biprism and its use for splitting and crossing two replicas of the pulse to be measured. It maps delay onto transverse position of the crystal.

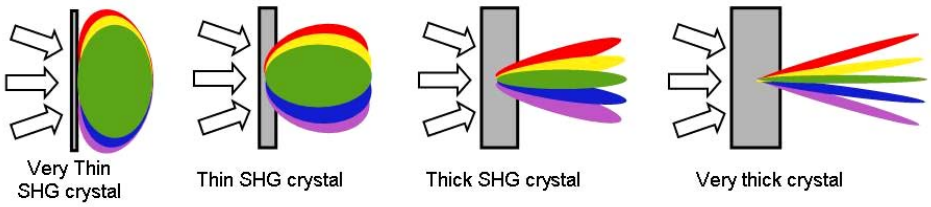

Fig. 2. (b). Rough polar plots of the output SHG intensity of a given color vs. angle for a tightly focused broadband input pulse and SHG crystals of various thicknesses. The thick crystal autocorrelates the tightly focused input pulse and simultaneously angularly disperses the resulting second-harmonic pulse.

#79262 - $15.00 USD Received 22 Jan 2007; revised 26 Mar 2007; accepted 27 Mar 2007; published 3 Apr 2007

As with all innovations, the Fresnel biprism and the thick crystal involve some subtlety[6]. For example, the Fresnel biprism should not be used for extremely short or long pulses. For short pulses, it can introduce too much group delay dispersion (GDD) and so must be replaced with a "Fresnel bimirror." For long pulses, a larger crossing angle is required to achieve the large range of delays, and the biprism apex angle becomes too small (i.e., far less than 180°), introducing too much angular dispersion in to the beams, and the beam may see very different GDD for different transverse positions. Its replacement with a Fresnel bimirror also has (geometrical) beam-crossing issues for long pulses. Nevertheless, the Fresnel biprism's physics is relatively simple, and it works well for a wide range of pulse lengths (~ 20 fs to ~ 1 ps), so we will not consider its effects here.

The thick crystal must also be used with care. Use of a thicker crystal yields better spectral resolution due to a smaller phase-matching bandwidth, but it also introduces more GDD into the pulse to be measured. Use of a thinner crystal does the opposite. Fortunately, the appropriate crystal thickness scales with the pulse length: a thinner crystal has less GDD and less spectral resolution, both appropriate for a shorter pulse. Nevertheless, the choice of the crystal thickness in GRENOUILLE is a careful compromise between opposing distortions. But just how touchy is this compromise? Specifically, how large a range of pulse lengths can be measured with a given crystal thickness? Ideally, the range should be about an order of magnitude or more for a single device.

In order to quantitatively answer this question, we must realize that the simple picture of Fig. 2(b) oversimplifies the potentially complex nonlinear optics somewhat. Not only is SHG occurring in the thick crystal, but a wide range of sum-frequency-generation (SFG) processes—both collinear and noncollinear—are also. So we must include these additional processes and check that this simple picture based only on SHG ideas accurately reflects the device's reality.

So in this paper we will numerically simulate GRENOUILLE measurements of ultrashort laser pulses, taking into account the above effects involving the thick crystal and the various SFG processes.

2. Numerical Simulation of GRENOUILLE

To simulate the second-order nonlinear-optical processes in GRENOUILLE, we work in $(\vec{k},\omega)$ space and assume the input beam is aligned along the z-axis, which is perpendicular to the crystal face. Because the input pulse is broadband, it involves a wide range of input frequencies (call a given pair ω_1 and ω_2) generating sum frequencies $\omega_3 = \omega_1 + \omega_2$ in a wide range of directions. Also, because the beams involved are tightly focused, each of these processes can also occur through off-axis phase-matching processes, $\vec{k}_1 + \vec{k}_2 = \vec{k}_3$, where $\vec{k}_3$ is the phase-matched sum frequency k-vector in a given direction.

Let *y* be the transverse direction in which the crystal's phase-matching wavelength varies. To simulate the physics of GRENOUILLE, we calculate the spectrum at the crystal exit face for each time delay and output angle in the *yz*-plane. For the *x*-dimension (the direction in which the delay between the two beams varies), we simply include a delay between the two pulse replicas. Under the non-depleted-pump assumption, we integrate the wave equation:

$$\frac{\partial E_3(k_{3y},\omega_3,z)}{\partial z} = \iint i\,\frac{d_{eff}\,\omega_3}{c\tilde{n}_3}\exp(-i\Delta k_z z)\times E_1(k_{1y},\omega_1,z)\,E_2(k_{3y}-k_{1y},\omega_3-\omega_1,z)\,dk_{1y}\,d\omega_1 \tag{1}$$

where E_3 is the sum-frequency field and $E_{1,2}$ correspond to the fundamental input fields. d_{eff} is the effective nonlinearity and $\tilde{n}$ is the effective refractive index. The field envelopes are constructed on a grid of (k_y,ω). The above-mentioned constraints $k_{3y} = k_{1y} + k_{2y}$ and $\omega_3 = \omega_1 + \omega_2$ are strictly enforced. The polarization at the generated sum frequency is

#79262 - $15.00 USD Received 22 Jan 2007; revised 26 Mar 2007; accepted 27 Mar 2007; published 3 Apr 2007

calculated for each (k_y, ω) taking into account the contribution from multiple $E_1(k_{1y}, \omega)$ and $E_2(k_{2y}, \omega)$ pairs that satisfy those conditions. The phase mismatch Δk_z is complicated and becomes a function of both frequency and off-axis angle with respect to *z*. For a Type I phase-matching process, considering a specific point $q_{(k_{3y},\omega_3)}$ on the grid (see Fig. 3), if we assume one of the suitable pairs that contributes is $P1_{(k_{1y},\omega_1)}$ and $P2_{(k_{2y},\omega_2)}$, the phase mismatch along *z*-axis Δk_{qz} for the grid point $q_{(k_{3y},\omega_3)}$ is computed by:

$$\Delta k_{qz} = \frac{\omega_3 n_e(\omega_3, \theta_3)}{c}\cos\theta_3 - \frac{\omega_1 n_o(\omega_1)}{c}\cos\theta_1 - \frac{\omega_2 n_o(\omega_2)}{c}\cos\theta_2 \qquad (2)$$

The angles θ_1, θ_2 and θ_3 can be easily calculated since they are fixed for each corresponding (k_y, ω) grid point. For the refractive indices, n_e and n_o, we used the full Sellmeier equation, so the crystal dispersion is included to all orders, rather than by an expansion in a power series. Then the radiation field contributed by $P1_{(k_{1y},\omega_1)}$ and $P2_{(k_{2y},\omega_2)}$ is simply $\propto iE_{p1}E_{p2}(\exp(-i\Delta k_{qz}L)-1)/\Delta k_{qz}$, where L is the length of the crystal.

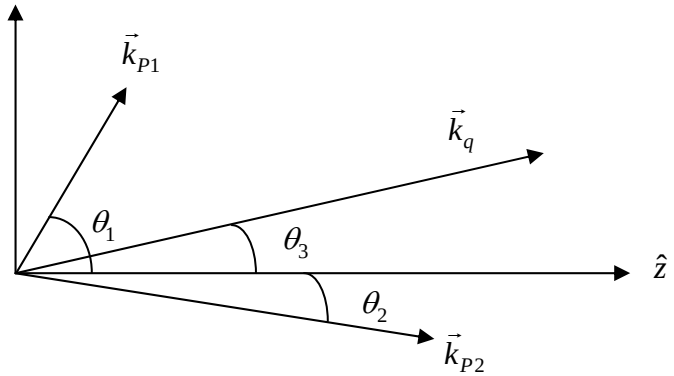

Fig. 3. Diagram for the phase-mismatch calculation. The k-vector of grid $q_{(k_{3y},\omega_3)}$ is tilted from the z-axis by θ_3. θ_1 and θ_2 are the tilt angles of the k-vectors of the electric field pair $P1_{(k_{1y},\omega_1)}$ and $P2_{(k_{2y},\omega_2)}$.

For our simulations, we use various temporal fields to test the device, but, in all cases, we assume a Gaussian-shaped spatial input-field profile. In addition, all the input beams are assumed to have their waists at the center of the crystal. For each delay between the two replicas, we integrate Eq. (1) to compute the SHG/SFG field. Because GRENOUILLE involves interpreting a given crystal output angle as the SHG frequency, we must compute the SHG/SFG intensity vs. crystal output angle, integrating over all frequencies. And because the focusing can be tight, we cannot simply interpret the transverse k-vector component, k_y, as the output angle. In other words, the off-axis k-vector component yields an output angle that also depends on the k-vector magnitude ($\sin\theta = k_y/[n_e(\omega,\theta)\omega/c]$).

To calibrate our simulated GRENOUILLE traces, we simulate a double pulse trace GRENOUILLE (FROG) trace, which has both well-known temporal and spectral structure that depends only on the pulse separation, as is done to calibrate GRENOUILLEs in practice[6]. The FROG retrieval algorithm is then applied to the computed GRENOUILLE trace, and the retrieved pulses are compared with the precise known input pulses.

We compare our simulated traces with ideal FROG traces, computed using the well-known formula:

#79262 - $15.00 USD Received 22 Jan 2007; revised 26 Mar 2007; accepted 27 Mar 2007; published 3 Apr 2007

$$I_{FROG}(\omega,\tau)=\left|\int_{-\infty}^{\infty}E(t)E(t-\tau)\exp(-i\omega t)\,dt\right|^2. \quad (3)$$

We also run the standard SHG FROG algorithm for our simulated GRENOUILLE traces and determine the accuracy with which GRENOUILLE determines both the SHG FROG trace and also, more importantly, the actual pulse. Our grid size for all traces is 128 x 128.

3. Results

3.1 Does GRENOUILLE yield the correct trace?

To determine whether GRENOUILLE correctly measures pulses in general, we performed simulations of several test pulses. We present a typical result here in which we simulated the GRENOUILLE trace of a 60-fs, flat-phase Gaussian, 800-nm input pulse (whose ideal FROG trace is shown in Fig. 4(a)). We use a 3.5 mm BBO SHG crystal, which is commonly used to measure pulses from 50 to about 500 fs in length. The input beam was focused to 10 μm in the center of the crystal. The delay increment used was 7.5591 fs, and the wavelength spacing was 0.5138 nm. The resulting GRENOUILLE trace is shown in Fig. 4(b), and the corresponding retrieved trace is shown in Fig. 4(c). The retrieved temporal and spectral intensities and phases show excellent agreement with the actual pulse temporal and spectral intensities and phases in Fig. 4(d) and (e). We find excellent agreement among the ideal, simulated, and retrieved traces. The root mean square (rms) error between the simulated GENOUILLE trace and the FROG trace was 0.007051. The rms error between the retrieved GRENOUILLE trace and the FROG trace was 0.006105. The rms error between the simulated and retrieved GRENOUILLE traces was 0.003534. In other words, the simulated and retrieved traces are quite accurate. Also, note that the rms error between the retrieved trace and the ideal FROG trace is less than that between the simulated trace and the ideal FROG trace. This is because the FROG algorithm is able to correct for slight discrepancies in the simulated (measured) trace due to the redundancy in the time-frequency-domain trace. We find that this occurs in all of our simulations and is a convenient feature of FROG (an effect we observe experimentally as well).

#79262 - $15.00 USD Received 22 Jan 2007; revised 26 Mar 2007; accepted 27 Mar 2007; published 3 Apr 2007

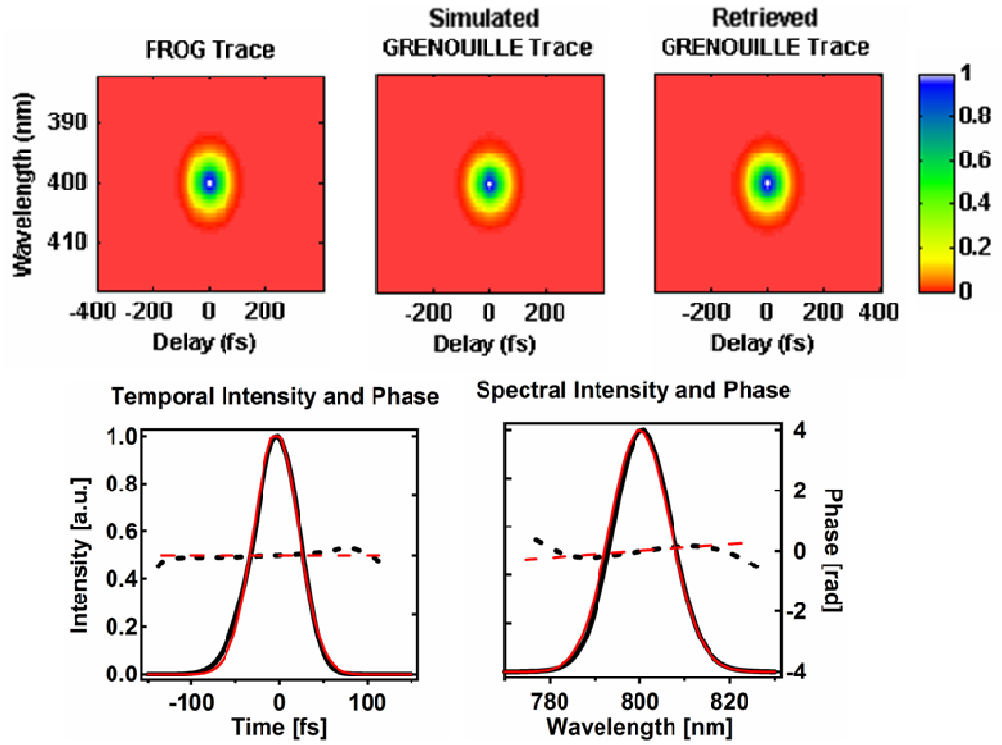

Fig. 4. (a) Ideal FROG trace for the 60fs flat phase pulse. (b) Simulated GRENOUILLE trace of a. (c) Retrieved GRENOUILLE trace. (d,e) The black lines show the retrieved temporal and spectral intensities and phases of the pulse. The red lines show the intensities and phases of the actual input pulse.

We also tested GRENOUILLE's ability to measure complex pulses, and we present one such example here. Figure 5 shows the ideal FROG trace, the simulated GRENOUILLE trace, and the retrieved trace for two overlapping chirped 50-fs pulses with identical parabolic phases (a "double chirped" pulse) using a 3.5 mm BBO crystal and 10 μm focal spot. The delay spacing was 9.4488 fs and wavelength spacing was 0.2509 nm. The rms error between the simulated GENOUILLE trace and the FROG trace was 0.006429. The rms error between the retrieved GRENOUILLE trace and the FROG trace was 0.006191. The rms error between the simulated and retrieved GRENOUILLE trace was 0.003383. We find that the simulated trace yields an intensity and spectrum that do not perfectly match the actual pulse, likely due to the finite beam divergence at the crystal, which yields a slight cropping of the spectrum, but they are not far off.

#79262 - $15.00 USD Received 22 Jan 2007; revised 26 Mar 2007; accepted 27 Mar 2007; published 3 Apr 2007

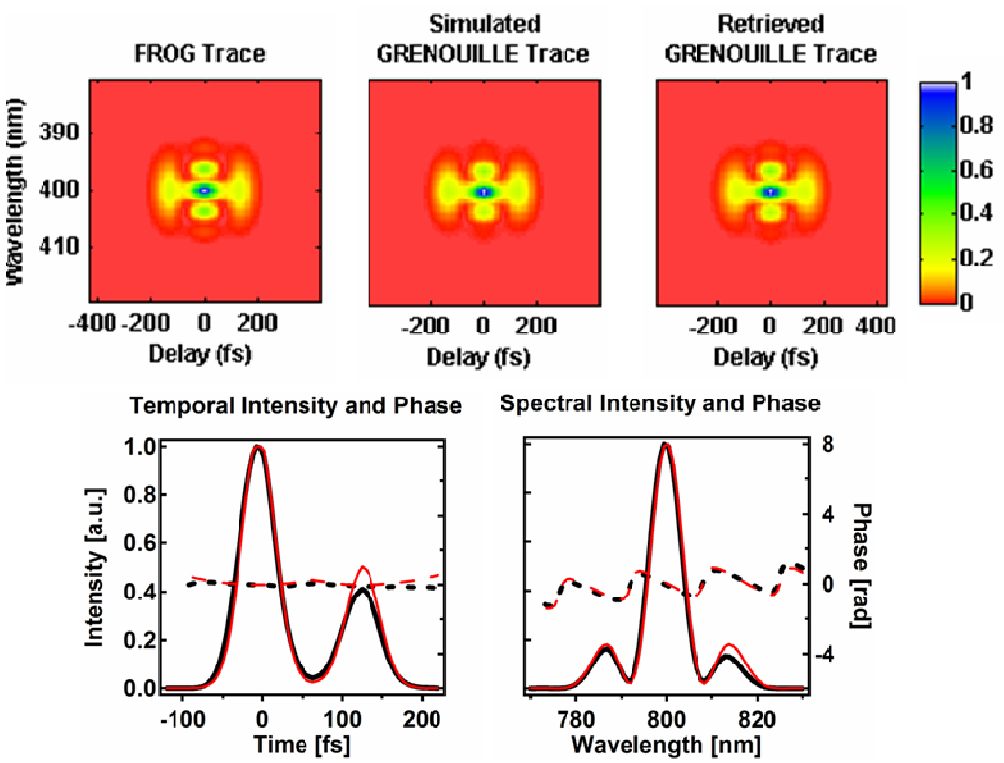

Fig. 5. (a) Ideal FROG trace of a double chirped 50 fs pulse. (b) Simulated GRENOUILLE trace. (c) Retrieved GRENOUILLE trace. (d,e) The black curves show the retrieved temporal and spectral intensities and phases of the pulse. The red curves show the intensities and phases of the actual input pulse.

3.2 Focusing issues

In GRENOUILLE, the thick crystal functions as the spectrometer dispersive element. Phase-matching maps SHG wavelength to output angle. This means that, in order to measure pulses with large bandwidths, the beam must have a large angular divergence, so a tight focus is required. A beam with too large a spot size and hence too little divergence will cause frequencies at the edges of the spectrum to be too weak in the resulting GRENOUILLE trace.

In the above simulation for the 60-fs pulse, if we were to use a larger focal spot with a correspondingly smaller angular divergence instead, an (erroneous) narrower spectrum would be obtained. And we see precisely this in our simulations, as shown in the movie in Fig. 6.

#79262 - $15.00 USD Received 22 Jan 2007; revised 26 Mar 2007; accepted 27 Mar 2007; published 3 Apr 2007

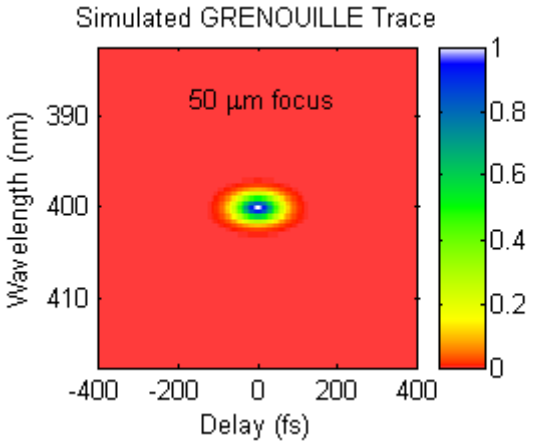

Fig. 6. (2.45 MB) Movie of simulated GRENOUILLE traces for a 60-fs flat-phase pulse focused at the center of a 3.5 mm BBO with different focal-length lenses. In the movie, the focal spot size evolves from 10 to 100 µm. The weaker foci yield traces that are spectrally too narrow.

3.3 Crystal thickness

Using a thicker crystal decreases the phase-matching bandwidth and so increases the GRENOUILLE spectral resolution. But the crystal should also not be too thick, or the pulse will spread in time due to the crystal GDD, and the pulse temporal structure will be lost. We simulate this effect by varying the crystal thickness and watching the simulated GRENOUILLE trace vary (See Fig. 7.). We use the same pulse as in Fig. 5.

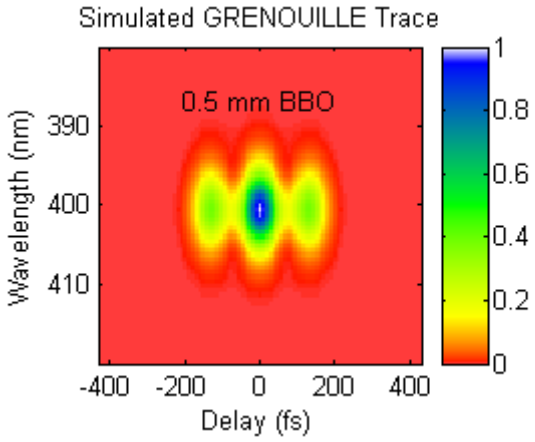

Fig. 7. (2.45 MB) Movie of simulated GRENOUILLE trace for a 50-fs double chirped pulse focused down to the center of a BBO crystal with a 10-µm focal spot. In the movie, the thickness of the BBO crystal changes from 0.5 mm to 9.5 mm.

Using a 0.5 mm BBO, the spectral fringes are almost completely lost. The temporal structure of the pulse becomes difficult to recognize for crystals longer than 7.5 mm. Some of the spectral side lobes in the FROG trace (See Fig. 5(a)) become quite fuzzy in the simulated

#79262 - $15.00 USD Received 22 Jan 2007; revised 26 Mar 2007; accepted 27 Mar 2007; published 3 Apr 2007

GRENOUILLE trace, as expected from a low-resolution spectrometer, ~ 2nm for this specific GRENOUILLE design.

3.3 Measurement of long and short pulses

The GRENOUILLE with the above mentioned configuration usually measures pulses ~ 50 to ~ 500 fs long. However, we find that measurements of pulses longer than 500 fs are also possible with very good accuracy. Figure 8 shows a case of a double chirped long pulse with structure in both delay and frequency and with pulse length of ~550 fs. A 3.5-mm BBO crystal was used with a 10-μm focal spot. The delay increment was 32.126 fs and the wavelength increment was 0.1589 nm. Interestingly, GRENOUILLE measures this pulse quite well. The rms error between the simulated GENOUILLE trace and the FROG trace was 0.021896, quite good for a pulse this complex. The rms error between the retrieved GRENOUILLE trace and the FROG trace was 0.015758. The rms error between the simulated and retrieved GRENOUILLE trace was 0.013183. Again, it appears that the well-known fundamental redundancy in the time-frequency-domain trace and the robust FROG phase-retrieval algorithm are able to compensate for the insufficient spectral resolution in the GRENOUILLE trace.

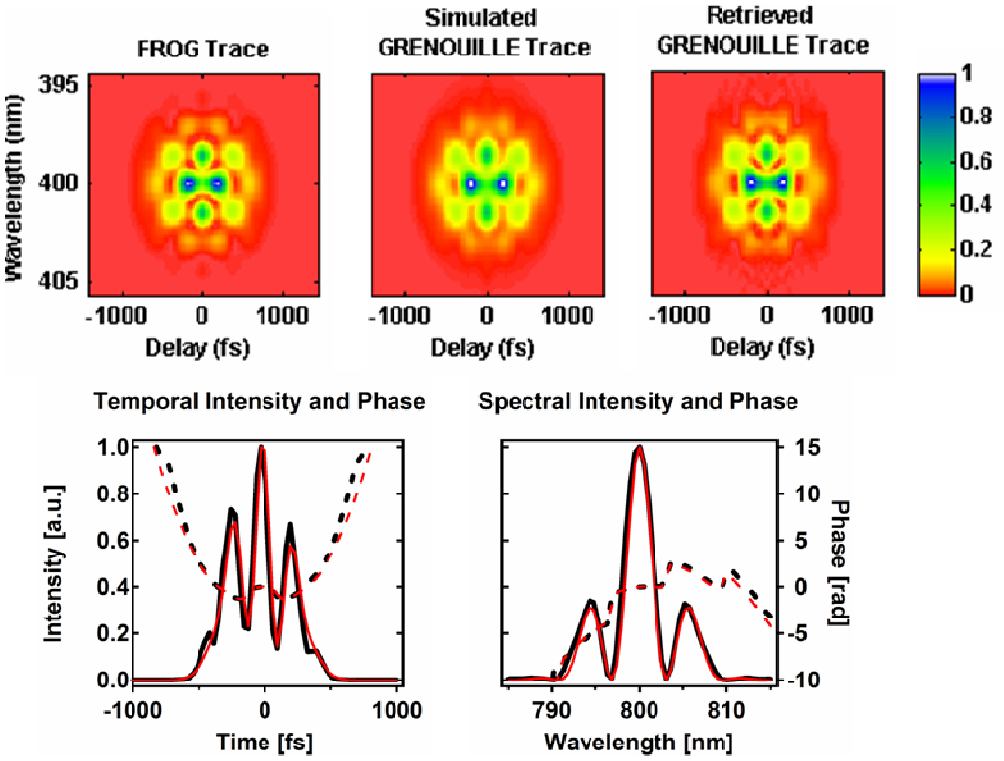

Fig. 8. (a) Ideal FROG trace of a double chirped long pulse. (b) Simulated GRENOUILLE trace of the same pulse. (c) Retrieved GRENOUILLE trace. (d,e) The black curves show the retrieved temporal and spectral intensities and phases of the pulse. The red curves show the intensities and phases of the actual input pulse.

The shortest pulses ever measured by GRENOUILLE are ~20 fs long [7]. The thickness of the BBO crystal in such measurements was 1.5 mm. A tighter focus ensured the larger

#79262 - $15.00 USD Received 22 Jan 2007; revised 26 Mar 2007; accepted 27 Mar 2007; published 3 Apr 2007

divergence angle required to cover the larger spectrum. The following simulation demonstrates GRENOUILLE's ability to measure pulses as short as 20 fs, which also have with fine structure (See Fig. 9.). We used a 5-μm focal-spot diameter. The delay increment used was 3.7795 fs and the wavelength spacing used was 1.4509 nm. The rms error between the simulated GENOUILLE trace and the FROG trace was 0.010379. The rms error between the retrieved GRENOUILLE trace and the FROG trace was 0.006799. The rms error between the simulated and retrieved GRENOUILLE trace was 0.008367. The intensities and phases versus time and frequency retrieve quite well. Pulse distortion due to material dispersion is negligible. The minor discrepancy is due to slightly insufficient resolution of the thick crystal 'spectrometer.'

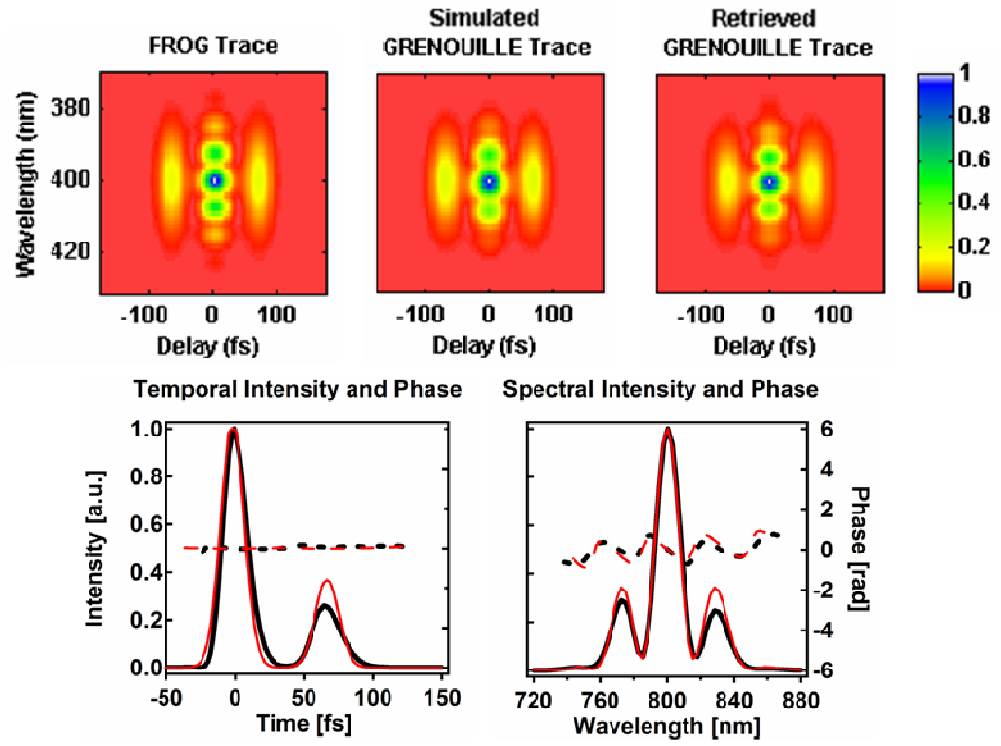

Fig. 9. (a) Ideal FROG trace of a slightly chirped 20 fs double pulse. (b) Simulated GRENOUILLE trace of this pulse. (c) Retrieved GRENOUILLE trace. (d,e) The black curves show the retrieved temporal and spectral intensities and phases of the pulse. The red curves show the intensities and phases of the actual input pulse.

This specific GRENOUILLE design has a resolution of ~ 4 nm at 800 nm, somewhat less than that required to resolve this relatively long pulse. Again, the FROG retrieval algorithm improves the trace, this time significantly (a factor of two improvement in the rms error), retrieving the spectral side lobes reasonably well.

For even shorter pulses, temporal broadening due to dispersion will be a problem (For BBO, 800nm type I phase matching, GVM(group velocity mismatch) = 1.92×10^3 fs/cm. The GDD(group delay dispersion)= 195.9 fs^2/mm at 400nm). However, a thinner crystal could be used in this case.

4. Conclusions

We have numerically simulated the performance of GRENOUILLE, which involves considering the complex sum-frequency generation of tightly focused, broadband input beams

#79262 - $15.00 USD Received 22 Jan 2007; revised 26 Mar 2007; accepted 27 Mar 2007; published 3 Apr 2007

in a thick SHG crystal. We take into account dispersion using the full Sellmeier equation. We have shown that using an appropriate crystal thickness and beam focus assures the accuracy of a GRENOUILLE measurement.

Specifically, our simulations show that GRENOUILLE is able to accurately measure pulses over at least an order of magnitude range of pulse lengths, spectral widths, and temporal and spectral structure. Despite its experimental simplicity, it is even capable of measuring complex pulses with time-bandwidth products approaching ~10. Only more complex, complete versions of FROG (and its cousin XFROG) can do better. Such performance, which matches that of GRENOUILLEs observed experimentally, is more than adequate for monitoring the output of today's ultrafast lasers and even measuring some shaped pulses.

#79262 - $15.00 USD Received 22 Jan 2007; revised 26 Mar 2007; accepted 27 Mar 2007; published 3 Apr 2007